

# Water proton spin saturation affects measured protein backbone $^{15}\text{N}$ spin relaxation rates

Kang Chen, Nico Tjandra \*

Laboratory of Molecular Biophysics, National Heart, Lung, and Blood Institute, National Institutes of Health, Bethesda, MD 20892, United States

## ARTICLE INFO

### Article history:

Received 26 May 2011

Revised 19 September 2011

Available online 1 October 2011

### Keywords:

Spin relaxation

Dephase

Flip-back

Saturation

Recovery time

Order parameter

## ABSTRACT

Protein backbone  $^{15}\text{N}$  NMR spin relaxation rates are useful in characterizing the protein dynamics and structures. To observe the protein nuclear-spin resonances a pulse sequence has to include a water suppression scheme. There are two commonly employed methods, saturating or dephasing the water spins with pulse field gradients and keeping them unperturbed with flip-back pulses. Here different water suppression methods were incorporated into pulse sequences to measure  $^{15}\text{N}$  longitudinal  $T_1$  and transversal rotating-frame  $T_1\rho$  spin relaxation. Unexpectedly the  $^{15}\text{N}$   $T_1$  relaxation time constants varied significantly with the choice of water suppression method. For a 25-kDa *Escherichia coli* glutamine binding protein (GlnBP) the  $T_1$  values acquired with the pulse sequence containing a water dephasing gradient are on average 20% longer than the ones obtained using a pulse sequence containing the water flip-back pulse. In contrast the two  $T_1\rho$  data sets are correlated without an apparent offset. The average  $T_1$  difference was reduced to 12% when the experimental recycle delay was doubled, while the average  $T_1$  values from the flip-back measurements were nearly unchanged. Analysis of spectral signal to noise ratios ( $s/n$ ) showed the apparent slower  $^{15}\text{N}$  relaxation obtained with the water dephasing experiment originated from the differences in  $^1\text{H}_\text{N}$  recovery for each relaxation time point. This in turn offset signal reduction from  $^{15}\text{N}$  relaxation decay. The artifact becomes noticeable when the measured  $^{15}\text{N}$  relaxation time constant is comparable to recycle delay, e.g., the  $^{15}\text{N}$   $T_1$  of medium to large proteins. The  $^{15}\text{N}$  relaxation rates measured with either water suppression schemes yield reasonable fits to the structure. However, data from the saturated scheme results in significantly lower Model-Free order parameters ( $\langle S^2 \rangle = 0.81$ ) than the non-saturated ones ( $\langle S^2 \rangle = 0.88$ ), indicating such order parameters may be previously underestimated.

Published by Elsevier Inc.

## 1. Introduction

Protein backbone  $^{15}\text{N}$  spin relaxation rates, the longitudinal ( $T_1$ ) and the transversal ( $T_2$ ) relaxation, are sensitive to the motion of protein N–H bond vectors. Accurately measured  $T_1$  and  $T_2$  are often used to derive both protein global diffusion parameters and local fast motions of the N–H bonds through numerical fitting, e.g. the Model-Free approach [1,2]. These parameters are useful in describing thermodynamic changes occurring in biomolecules as they function. In addition, since the ratio  $T_1/T_2$  has been demonstrated to be dependent on the projection of the individual N–H bond to the protein rotational diffusion tensor frame [3], they can be applied as restraints to refine structures [4–6], as well as to relatively position domains within a protein complex [7–10]. The  $T_1/T_2$  restraints are readily available and could be very helpful in characterizing larger systems. In contrast other NMR restraints are either requiring special treatment of the sample to measure, e.g.

residual dipolar couplings (RDC) [11–13] and paramagnetic relaxation enhancement (PRE) [14], or not measurable, i.e. NOEs in deuterated system.

Similar to other solution NMR experiments accurate measurements of  $^{15}\text{N}$   $T_1$  and  $T_2$  require satisfactory suppression of water  $^1\text{H}$  signals. One approach is to dephase or saturate water  $^1\text{H}$  spin coherence with the use of pulse field gradient or composite pulses [15–19]. Alternatively flip-back pulses, which keep water proton spins parallel to the  $B_0$  field throughout the pulse sequence, became popular owing to the advantage in minimizing effects of radiation damping on cryogenic probes [20,21]. Here we have incorporated both water suppression schemes into 2D  $^1\text{H}$ – $^{15}\text{N}$  pulse sequences for measuring  $^{15}\text{N}$   $T_1$  and  $T_1\rho$ . Significantly longer  $T_1$  values were obtained when water proton spins were saturated by the gradient. Close analysis of relaxation curves and spectral signal to noise ( $s/n$ ) ratio illustrated that the  $^{15}\text{N}$  relaxation difference originated from the varied  $^1\text{H}_\text{N}$  recovery caused by water saturation. The conclusion was supported by the fact that doubling the recycle delay reduced the relaxation rate differences. Interestingly such  $^{15}\text{N}$  relaxation rate discrepancies did not produce any noticeable differences in their fit to the rotational diffusion tensor, however, the derived order parameters differed significantly. Thus

\* Corresponding author. Address: Building 50, Room 3503, National Heart, Lung, and Blood Institute, National Institutes of Health, Bethesda, MD 20892, United States. Fax: +1 301 402 3405.

E-mail address: [tjandra@nhlbi.nih.gov](mailto:tjandra@nhlbi.nih.gov) (N. Tjandra).

saturating water proton spins causes artifacts in measuring  $^{15}\text{N}$  relaxation rates, which also affect the interpretation of fast motion dynamics.

## 2. Results

### 2.1. Pulse sequences

The 2D  $^1\text{H}$ – $^{15}\text{N}$  ST2-PT TROSY pulse sequence [22–24] was modified to include relaxation delays (Fig. 1). Shown in Fig. 1a is the pulse sequence for measuring longitudinal  $T_1$  relaxation. Pulses between points *b* and *c* in Fig. 1a are replaced with pulses in Fig. 1b to measure the transverse rotating frame relaxation  $T_{1\rho}$ . At point *a* of Fig. 1a the two-spin order  $H_2N_2$  is established and water proton spins are on the transverse plane. For the water flip-back version of the measurement the soft 1.2-ms long  $^1\text{H}$  pulse, the open rectangle in Fig. 1a, was applied to flip water proton spins to +*z*. The in-phase  $N_x$  component was established at point *b* for the relaxation delays. Proton water-gate pulses, which flip non-water proton spins 180°, were applied periodically during  $T_1$  and  $T_{1\rho}$  relaxation delays to cancel cross-correlations [25]. At point *c* gradient pulse  $G_5$  is a *z*-filter to clean any transverse magnetizations. Shaped and water-gate proton pulses were implemented during the TROSY detection to ensure water spins stay on +*z* (Fig. 1a).

The dephase version of the pulse sequences stay nearly identical to the flip-back ones described above except for replacing the soft 1.2-ms long  $^1\text{H}$  pulse (the open rectangle in Fig. 1a) with a 1.2-ms delay. Such modification allows water proton spin coherence to be destroyed by the gradient pulse  $G_3$ . Other than the difference of this soft  $^1\text{H}$  pulse, the rest of the pulse sequence remains identical between the two water suppression schemes so that any imperfection in canceling  $^1\text{H}$ – $^{15}\text{N}$  cross-correlation would affect the two measurements equally.

### 2.2. Measured $T_1$ and $T_{1\rho}$

The protein used to test the pulse sequences is *Escherichia coli*. Glutamine Binding Protein (GlnBP), which has a total of 226 residues and is highly anisotropic with a moment inertia ratio of 2. Chemical shift assignments of a total of 211 out of 219 non-proline  $^1\text{H}$ – $^{15}\text{N}$  resonances [26] were confirmed using conventional 3D experiments. Amide proton of residues undergoing exchange, A1,

D2, G21, D22, D73, N97, N99, and G171, could not be observed. Overlapping residues E74, F136, L146, L196, K199, and K205 were further excluded, and 205 resonances were left for analysis. The NMR sample of 250  $\mu\text{M}$   $^2\text{H}/^{15}\text{N}$  labeled GlnBP was subject to relaxation measurements under either of the two water suppression schemes (Fig. 1) at 34 °C and a magnetic field of 14.1 T.

For  $T_1$  measurements the average curve fitting errors for the exponential decay function were 1.3% and 1.8% for dephase and flip-back data sets, respectively. Our experimental reproducibility error was 2.4%. The correlation plots of  $T_1$  from two different water suppression schemes (Fig. 2a) indicated significant differences between the two data sets with a large r.m.s.d. value of 181 ms between the two, or about 21% of the average  $T_1$  of the flip-back data set, which was 869.4 ms. Residues with side-chain being exposed [27] were indicated (Fig. 2a) and there was no correlation between surface exposure and  $T_1$  differences. The dephase pulse sequence which saturated water magnetizations resulted in a significantly slower  $T_1$  relaxation.

For  $T_{1\rho}$  the average curve fitting errors were 1.6% and 1.5% for dephase and flip-back data sets, respectively, and the r.m.s.d. between the two was 2.46 ms, about 3.4% of the average  $T_{1\rho}$  of the flip-back data set, which was comparable to the reproducibility error of 3.0%. In fact the  $T_{1\rho}$  correlation plot in Fig. 2b shows a much better agreement between the two measurements under different water suppression schemes than  $T_1$ s in Fig. 2a. Similarly surface exposed residues do not differentiate from others.

### 2.3. $^{15}\text{N}$ relaxation rate differences and spectra *s/n*

Resonance intensities of  $^{15}\text{N}$   $T_1$  and  $T_{1\rho}$  relaxation data points for a buried residue A96 were plotted (Fig. 3). Overall the peak intensities for dephase measurements are significantly lower than flip-back ones due to saturation on water  $^1\text{H}$  and protein  $^1\text{H}_\text{N}$  spins. For all relaxation time points in  $T_{1\rho}$  experiments there is a relatively constant 50% reduction of peak intensities in the dephase measurement (Fig. 3b). And the fit of  $T_{1\rho}$  relaxation time constants from the two measurements are within 1.1%. However, for  $T_1$  experiments such peak intensity reduction is not uniform for all time points (Fig. 3a), and the fit  $T_1$  relaxation time constants differs by 30%. The varied peak intensity ratio of  $T_1$  points indicated the initial  $^1\text{H}_\text{N}$  magnetization population was not uniform within the water saturation experiment. The longer the  $T_1$  relaxation delay

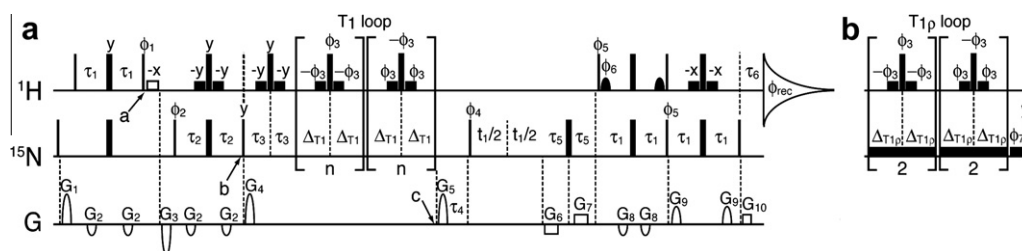


**Fig. 1.** The 2D  $^1\text{H}$ – $^{15}\text{N}$  pulse sequences for measuring  $^{15}\text{N}$  spin relaxation time constants  $T_1$  (a) and  $T_{1\rho}$  (b) under TROSY detection. The pulses in panel 1a between points *b* and *c* are replaced with pulses in panel 1b to establish the pulse sequence for  $T_{1\rho}$  measurement. The  $^1\text{H}$  and  $^{15}\text{N}$  carrier frequency was set to 4.663 ppm and 118.1 ppm, respectively. Narrow and wide filled rectangles correspond to hard pulses with flip angles of 90° and 180°, respectively. The open rectangle at point *a* is a 1.2-ms long 90° square pulse, turned on and off for water flip-back and dephase measurements, respectively. Other low-power filled squares on  $^1\text{H}$  channel are 90° square pulses with a width of 1.0 ms. Filled bells are 90° sinc-shaped water-selective pulses with a duration of 1.9 ms. In panel 1b the spin lock (SL) and the following 2-ms purge pulses on  $^{15}\text{N}$  channel had a  $\gamma B_1$  field strength of 2000 Hz and were applied with phase  $\phi_7$ . Pulses are *x*-phase by default. Phase cycles are listed as follows,  $\phi_1 = 4(y)$ ,  $4(-y)$ ;  $\phi_2 = 8(x)$ ,  $8(-x)$ ;  $\phi_3 = 16(y)$ ,  $16(-y)$ ;  $\phi_4 = y$ ,  $-y$ ,  $x$ ,  $-x$ ;  $\phi_5 = y$ ;  $\phi_6 = -y$ ;  $\phi_7 = 32(x)$ ,  $32(-x)$ ;  $\phi_{\text{rec}} = y$ ,  $-y$ ,  $x$ ,  $-x$ ,  $2(-y)$ ,  $y$ ,  $-x$ ,  $x$ ,  $y$ ,  $-y$ ,  $x$ ,  $-x$ . Delay durations are listed as follows,  $\tau_1 = 2.3$  ms,  $\tau_2 = 2.7$  ms,  $\tau_3 = 2$  ms,  $\tau_4 = 15$  ms,  $\tau_5 = 0.4$  ms,  $\tau_6 = 0.08$  ms,  $\Delta T_1 = 4.0$  ms. All gradient pulses are along *z*-axis and  $G_6$ ,  $G_7$ , and  $G_{10}$  are in rectangular shape while the rest are sine-shaped. The duration, sign and strength for gradient pulses are as follows,  $G_1 = 3$  ms, 15 G/cm;  $G_2 = 1$  ms,  $-7.5$  G/cm;  $G_3 = 2$  ms,  $-25$  G/cm;  $G_4 = 1$  ms, 25 G/cm;  $G_5 = 2$  ms, 25 G/cm;  $G_6 = 200$   $\mu\text{s}$ ,  $-15$  G/cm;  $G_7 = 200$   $\mu\text{s}$ , 15 G/cm;  $G_8 = 0.25$  ms,  $-9$  G/cm;  $G_9 = 1$  ms, 15 G/cm;  $G_{10} = 40.5$   $\mu\text{s}$ , 15 G/cm. Quadrature detection on the  $^{15}\text{N}$  dimension was achieved via Echo-Antiecho method [49–51] such that the second fid for each increment of  $t_1$  was collected with signs of gradient pulses  $G_6$  and  $G_7$  being switched, and pulse phases of  $\phi_4 = y$ ,  $-y$ ,  $-x$ ,  $x$ ,  $\phi_5 = -y$ , and  $\phi_6 = y$  being applied. For  $T_1$  measurement the relaxation delay equals  $\Delta T_1 \times 4 \times n$  where the loop number  $n$  was varied to yield different relaxation delays. For  $T_{1\rho}$  measurement the relaxation delay equals total SL-duration,  $\Delta T_{1\rho} \times 8$ , and  $\Delta T_{1\rho}$  was varied. For  $T_1$  measurement gradient pulse  $G_4$  is a *z*-filter to clean any magnetization other than  $N_z$ . For  $T_{1\rho}$  measurement the  $^{15}\text{N}$  spin lock pulse was extended for 2 ms after the relaxation blocks to completely remove any component not in the direction of the spin lock (Fig. 1b); the  $^{15}\text{N}$  spin was then restored to the *z* direction by a 90°(*y*) pulse.

Download English Version:

<https://daneshyari.com/en/article/5406094>

Download Persian Version:

<https://daneshyari.com/article/5406094>

[Daneshyari.com](https://daneshyari.com)